



Measurement of the ${}^7\text{Li}(p,p'\gamma){}^7\text{Li}$ reaction cross-section and 478 keV photon yield from a thick lithium target at proton energies from 0.7 to 1.85 MeV

Timofey Bykov^{a,b}, Dmitrii Kasatov^{a,b}, Iaroslav Kolesnikov^{a,b}, Alexey Koshkarev^{a,b}, Alexandr Makarov^{a,b}, Ivan Shchudlo^{a,b}, Evgeniia Sokolova^{a,b}, Sergey Taskaev^{a,b,*}

^a Budker Institute of Nuclear Physics, Novosibirsk, Russia

^b Novosibirsk State University, Novosibirsk, Russia

ARTICLE INFO

Keywords:

Accelerator based boron neutron capture therapy
Cross-section
Photon yield
Lithium target

ABSTRACT

The ${}^7\text{Li}(p,p'\gamma){}^7\text{Li}$ reaction cross section and photon yield from a thick lithium target at proton energies from 0.7 to 1.85 MeV have been measured with a HPGe gamma-ray spectrometer. The spectrometer is calibrated on total and relative sensitivity by reference radionuclide sources of photon radiation. The measurement results are compared with those presented in the EXFOR nuclear reaction database and with other data published in open sources. The reliability of the results of previous studies is analyzed.

1. Introduction

Boron neutron capture therapy (BNCT) (Sauerwein et al., 2012) which requires an intensive epithermal neutron beam is considered to be a promising technique for treatment of malignant tumors. It is generally recognized that the generation of neutrons as a result of the ${}^7\text{Li}(p,n){}^7\text{Be}$ threshold reaction at proton energies in the region of 2.3–2.5 MeV allows forming a neutron beam that best meets the requirements of BNCT (IAEA-TECDOC-1223, 2001; Zaidi et al., 2018). An epithermal neutron source (Bayanov et al., 1998; Taskaev, 2015, 2019) consisting of a vacuum insulated tandem accelerator for proton beam production and a lithium target for neutron generation has been proposed and created at Budker Institute of Nuclear Physics. The target is made as a thin¹ lithium layer evaporated on an efficiently cooled copper substrate (Bayanov et al., 2004, 2006).

Accompanying photon absorbed dose is undesirable for BNCT but it arises inevitably. It is known that as a result of inelastic proton scattering 478 keV photons are emitted from lithium nuclei. Total photon absorbed dose includes this dose together with other doses from photons emitted by ${}^7\text{Be}$ decay, from neutron capture by hydrogen nuclei and by a number of atomic nuclei that are part of structural materials. Knowing the

photon yield of the ${}^7\text{Li}(p,p'\gamma){}^7\text{Li}$ reaction is certainly important for nuclear data evaluation and for estimating the absorbed dose during therapy planning. However, the data of the 478 keV photon yield and the data of the ${}^7\text{Li}(p,p'\gamma){}^7\text{Li}$ reaction cross section in the literature (Antilla et al., 1981; Kononov et al., 1997; Savidou et al., 1999; EXFOR experimental nuclear reaction database; Saito et al., 2017; Brown et al., 1951; Mozer et al., 1954; Presser et al., 1972; Mateus et al., 2002) differ significantly. Fig. 1 shows the data of 478 keV photon yield in the ${}^7\text{Li}(p,p'\gamma){}^7\text{Li}$ reaction, and Fig. 2 shows the data of the ${}^7\text{Li}(p,p'\gamma){}^7\text{Li}$ reaction cross section.

The aim of this work is to measure cross-section of the ${}^7\text{Li}(p,p'\gamma){}^7\text{Li}$ reaction and 478 keV photon yield from a thick lithium target at proton energies below the ${}^7\text{Li}(p,n){}^7\text{Be}$ reaction threshold.

1.1. Experimental setup

The study was carried out on a vacuum insulated tandem accelerator (Taskaev, 2015, 2019) at proton beam energies from 0.7 to 1.85 MeV and a current of 300 μA . The scheme of the experimental setup is shown in Fig. 3. In accelerator 1, a low-energy beam of negative hydrogen ions are generated by the source 1a, focused by the magnetic lenses 1b to the

* Corresponding author. Budker Institute of Nuclear Physics, 11 Lavrentiev ave., 630090, Novosibirsk, Russia.

E-mail addresses: taskaev@inp.nsk.su, taskaev.sergey@gmail.com (S. Taskaev).

¹ The term “thin” means that protons pass through the lithium and are absorbed in the metal on which the lithium is deposited. For the generation of neutrons, it is optimal that the proton energy at the exit from the lithium layer is equal to or slightly below 1.882 MeV – the threshold of the ${}^7\text{Li}(p,n){}^7\text{Be}$ reaction. For the generation of 478 keV photons, the target will be thick if the proton energy at the exit from the lithium layer is below 0.478 MeV – the threshold of the ${}^7\text{Li}(p,p'\gamma){}^7\text{Li}$ reaction.

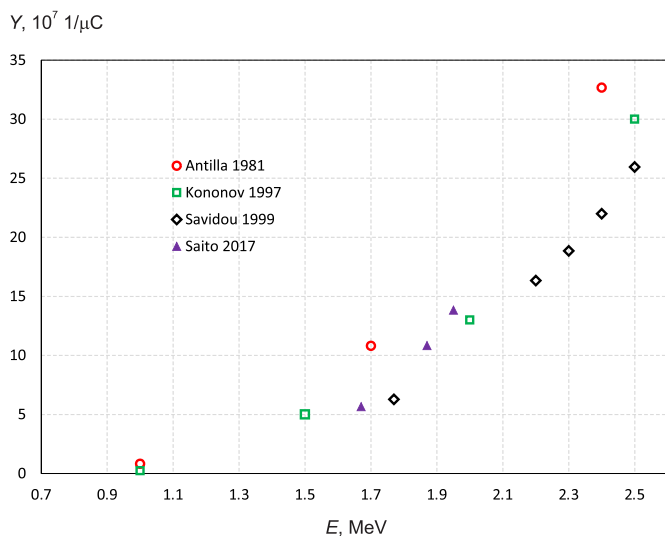


Fig. 1. Yield of 478 keV photon in the ${}^7\text{Li} (p,p'\gamma){}^7\text{Li}$ reaction: \circ - measured (Antilla et al., 1981), \square - calculated (Kononov et al., 1997), \diamond - measured at $E = 1.75$ MeV and calculated at other energy values (Antilla et al., 1981), Δ - measured at $E = 1.67$ MeV and 1.87 MeV and estimated at 1.95 MeV (Saito et al., 2017).

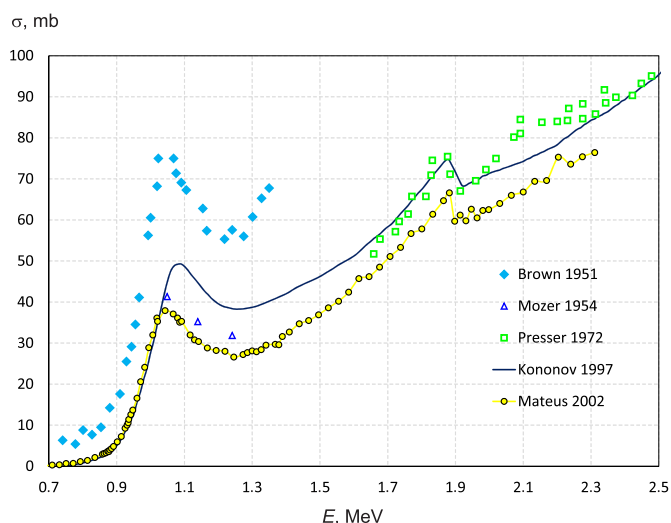


Fig. 2. ${}^7\text{Li} (p,p'\gamma){}^7\text{Li}$ reaction cross-section from (Brown et al., 1951; Mozer et al., 1954; Presser et al., 1972; Kononov et al., 1997; Mateus et al., 2002). (For interpretation of the references to colour in this figure legend, the reader is referred to the Web version of this article.)

accelerator input port $1c$, and accelerated to an energy of 0.35–0.925 MeV. In the gas stripper $1d$ installed inside the central high-voltage electrode $1e$, negative hydrogen ions are stripped to protons, which are further accelerated to an energy of 0.7–1.85 MeV by the same high-voltage potential. Potentials of the high-voltage electrode $1e$ and the intermediate electrodes $1f$ are set from the high-voltage power supply $1h$ (not shown) through the high voltage feedthrough insulator $1g$. Then the proton beam is directed to the lithium target.

The lithium target 10 is placed at the end of the vacuum chamber 9 in the horizontal part of the proton beam transporting channel. The target is a copper disk with a diameter of 144 mm and 8 mm thick. On the proton beam side, a layer of lithium with a crystal density of 82 mm in diameter is thermally evaporated onto the copper disc. On the reverse side of the copper disk inside 122 mm diameter four spiral-shaped channels for water cooling have been made (Bayanov et al., 2006). A

flat aluminum disk with holes for the cooling water supply and outlet is pressed against this side of the copper disk. At a typical water flow of 15–17 l/min, a turbulent water flow with a speed of 3.5–4 m/s is realized in the cooling channels, which provides effective heat removal (Bayanov et al., 2004). Vacuum evaporation of lithium on the copper disc is carried out at a separate stand according to the scenario similar to that described in (Bayanov et al., 2008). After lithium deposition, the target unit together with a part of vacuum chamber 9 closed with a gate valve to maintain vacuum inside is disconnected from the lithium evaporation stand, transferred to the experimental facility and connected to the horizontal proton beam transporting channel.

A proton beam of 1 cm diameter is obtained on a vacuum insulated tandem accelerator 1 . Proton current is measured and controlled by a non-destructive DC current transformer NPCT (Bergoz Instrumentation, France) 3 ; the position of the beam is measured by thermocouples inserted inside the cooled diaphragms 2 . The position and size of the proton beam on the surface of the lithium target 10 are measured and controlled by the Hikvision video camera installed on the window 14 and eight thermocouples inserted into the holes inside the target 10 drilled from the side surface of the copper disc.

The intensity of gamma radiation is measured by the gamma-ray spectrometer SEG-1KP-IPTP 12 (Institute of Physical and Technical Problems, Dubna, Russia) 12 based on a semiconductor detector made of extremely pure germanium (HPGe gamma-ray spectrometer). The sensitive part of the spectrometer is located at a distance of 2.00 m at an angle of 110° . The spectrometer is placed inside the lead collimator 13 with external diameter of 270 mm, 500 mm length and 50 mm wall thickness. Together with the collimator, the spectrometer is protected from a bremsstrahlung of the accelerator by a 23 cm thick wall 11 built of concrete blocks. Note that the location of the concrete wall, collimator and spectrometer is shown in Fig. 3 schematically; in reality they are located in the horizontal plane behind a vacuum chamber with a lithium target.

A typical signal of the HPGe gamma-ray spectrometer is shown in Fig. 4. It shows a narrow useful signal in the region of 478 keV, a broad signal due to bremsstrahlung of the accelerator, the intensity of which increases with increasing accelerator voltage, and in the region below 90 keV characteristic X-rays emitted by lead. The dead time of the spectrometer did not exceed 26% when measuring the reaction cross section and 13.4% when measuring the photon yield.

HPGe gamma-ray spectrometer is calibrated on total sensitivity by closed type Cs-137 radionuclide source of photon radiation with activity $1.6 \cdot 10^8$ Bq (10% accuracy) in 661.657 keV line. During calibration the radionuclide source was placed on the surface of the copper disk in its center – as close as possible to the lithium layer. The relative sensitivity of the HPGe gamma-ray spectrometer was calibrated by the following reference sources of photon radiation from the OSGI-TR set (Ritverc, Russia): Na-22, Mn-54, Co-60, Ba-133, Cs-137, Eu-152 and Bi-207. Intensity reliability of reference radiation sources is 7%. Finally, the absolute efficiency at 478 keV was fixed by interpolating the data obtained.

2. Results and discussion

2.1. 478 keV photon yield from a thick lithium target measurement

The experimental result of the 478 keV photon yield from a thick lithium target at proton energies from 0.7 to 1.85 MeV with 25 keV steps is presented in Fig. 5. The lower energy limit is determined by the possibility of the accelerator, the upper one – by the impossibility to use the HPGe gamma-ray spectrometer in the neutron field due to dislocations arising in the detector crystal. The target is called thick if the thickness of the evaporated lithium layer exceeds the proton range in lithium. The proton range is equal to 31 μm at proton energy 0.7 MeV and 144 μm at 1.85 MeV (Andersen and Ziegler, 1997). In the experiments performed, the lithium thickness was 200 μm .

Energy stability during the experiment was between 0.1 and 0.2%, average 0.14%. The absolute value of energy was calibrated according to the threshold of generation of neutrons of the ${}^7\text{Li} (p,n){}^7\text{Be}$ reaction equal to 1.882 MeV. The 478 gamma rays were measured for 2 min at each points, so that the error in measuring the count rate does not exceed 0.5%. Approximately the same measurement error was produced at measuring the charge carried by the proton beam, while the current stability of the proton beam was 3%. As a result, the measurement error of the relative value of the photon yield shown in Fig. 5 did not exceed 1%. Measurement of the absolute photon yield is performed using a closed type Cs-137 radionuclide source of photon radiation, whose intensity reliability is 10%, and reference sources of photon radiation from the OSGI-TR set, whose intensity reliability is 7%. Summing up, we can say that the absolute gamma-ray yield from a thick lithium target is measured with better than 15% accuracy. Note that in Fig. 5 the vertical error bars only show a relative error not exceeding 1%; the absolute error, not shown in the figure, is 15%.

Let us compare the obtained result with those previously measured and calculated. In (Antilla et al., 1981) the measured gamma-ray yield is given equal to $0.817 \cdot 10^7 \mu\text{C}^{-1}$ at 1 MeV, which is 1.67 times more than we measured, and $10.8 \cdot 10^7 \mu\text{C}^{-1}$ at 1.7 MeV, which is 1.78 times more than we measured. In (Kononov et al., 1997) the calculated yield of gamma rays is given as $0.24 \cdot 10^7 \mu\text{C}^{-1}$ at 1 MeV, which is 2 times less than we measured, and $5 \cdot 10^7 \mu\text{C}^{-1}$ at 1.5 MeV, which is 1.3 times more than we measured. In (Savidou et al., 1999) the measured yield of gamma-ray quanta is given as $6.283 \cdot 10^7 \mu\text{C}^{-1}$ at 1.77 MeV, which is 13% less than the value at 1.77 MeV extrapolated from our measurements. In (Saito et al., 2017) the measured yield of gamma-ray quanta is given as $5.66 \pm 0.2 \cdot 10^7 \mu\text{C}^{-1}$ at 1.67 MeV, which is equal to our measured $5.77 \pm 0.07 \cdot 10^7 \mu\text{C}^{-1}$ at 1.672 ± 0.002 MeV.

The dependence of the 478 keV photon yield on the proton energy measured with a relative accuracy better than 1%, makes it possible to measure the thickness of lithium if its thickness is less than 100 μm (Kasatov et al., 2020).

2.2. Measurement of the ${}^7\text{Li}(p,p'\gamma){}^7\text{Li}$ reaction cross-section

Then in order to measure the cross-section of the ${}^7\text{Li} (p,p'\gamma){}^7\text{Li}$ reaction a thin layer of lithium was evaporated on the copper disk and the yield of 478 keV photons was measured at proton energies from 0.7 to 1.85 MeV with the same 25 keV energy steps in the same experimental geometry.

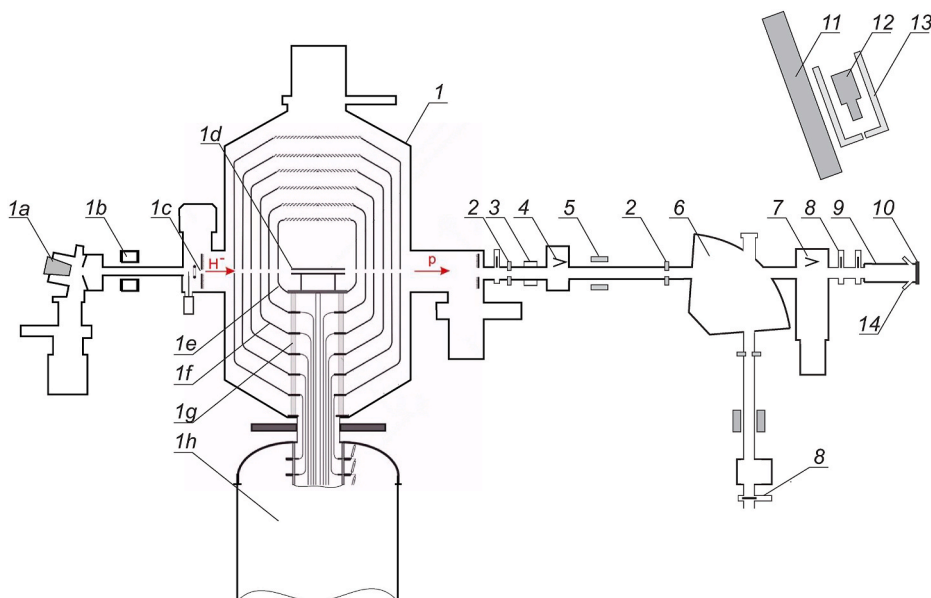


Fig. 3. Scheme of the experimental setup: 1 – vacuum insulated tandem accelerator (1a – negative hydrogen ion source, 1b – magnetic lenses, 1c – accelerator input port, 1d – gas stripper, 1e – central high-voltage electrode, 1f – intermediate electrodes, 1g – feedthrough insulator, 1h – high-voltage power supply), 2 – cooled 26 mm diaphragm, 3 – non-destructive DC current transformer, 4 – diagnostic chamber with inserted Faraday cup, 5 – corrector, 6 – bending magnet, 7 – diagnostic chamber with inserted Faraday cup and vacuum pumping, 8 – gate valve, 9 – vacuum chamber with gate valve, 10 – lithium target, 11 – concrete wall, 12 – gamma-ray spectrometer, 13 – lead collimator, 14 – view port.

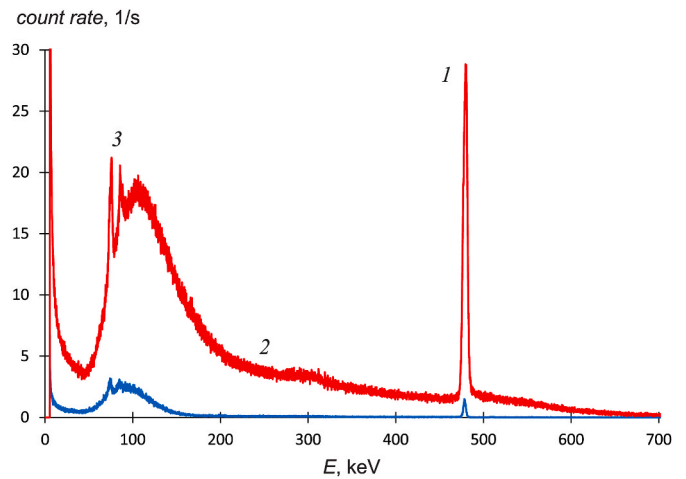


Fig. 4. Typical signal of HPGe gamma-ray spectrometer: 1 – 478 keV photons emitted in ${}^7\text{Li} (p,p'\gamma){}^7\text{Li}$ reaction, 2 – bremsstrahlung of the accelerator, 3 – characteristic X-rays emitted by lead. The upper curve was obtained at a proton energy of 1.75 MeV, the lower one – 0.8 MeV.

Since we are using a vapor deposition process to produce the target, the correct thickness is not known. The thickness of the lithium layer is defined as follows. It is known that the rate of proton energy loss S in lithium depends on its energy E as follows (Andersen and Ziegler, 1997):

$$S = \frac{S_{low} \cdot S_{high}}{S_{low} + S_{high}} \text{ eV} / (10^{15} \text{ atoms/cm}^2),$$

where $S_{low} = 1.6E^{0.45}$, $S_{high} = \frac{725.6}{E} \ln \left(1 + \frac{3013}{E} + 0.04578E \right)$, E is taken in keV. Using this formula, let us calculate the amount of proton energy loss in lithium with crystal density. We obtain that passing the lithium layer with 1 μm thickness the proton loses 15.4 keV at 0.7 keV and 7.77 keV at 1.85 MeV. The photon yield from a thin lithium target is $Y_x = n x \sigma I/e$, where x is the thickness of lithium, n is the density of lithium atomic nuclei ($4.59 \cdot 10^{22} \text{ cm}^{-3}$), σ is the ${}^7\text{Li} (p,p'\gamma){}^7\text{Li}$ reaction cross-section, I is the current of the proton beam, e is the elementary charge. Since the 478 keV line count rates on a thin and thick targets were measured in 25 keV steps in the same experimental geometry, the count rate Y_j of gamma quanta from a thick target can be determined

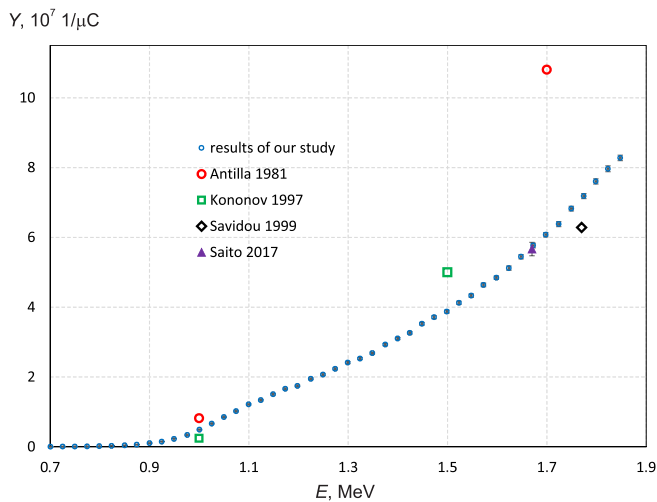


Fig. 5. Measured yield of 478 keV photons from a thick lithium target in the ${}^7\text{Li}(\text{p,p}'\gamma){}^7\text{Li}$ reaction. For comparison, the measurement data are given: \circ - (Antilla et al., 1981), \diamond - (Antilla et al., 1981), Δ - (Saito et al., 2017) and calculations: \square - (Kononov et al., 1997).

from the measured count rate Y_i from a thin target as $Y_j = \sum_{i=0}^j Y_i \frac{25}{S_i(x)}$, where the index i indicates the measurement number ($i = 0$ at 0.7 MeV, $i = 1$ at 0.725 MeV and so on in 25 keV increments), $S_i(x)$ – the value of the proton energy loss (in keV) in a lithium layer with thickness x . Fig. 6 presents two curves of the count rate from a thick target, one measured, and another reconstructed by the above formula with a thickness of lithium of 2.1 μm . In this case, the measured and reconstructed curves are the best match, which means that lithium thickness is $2.10 \pm 0.03 \mu\text{m}$.

Since the lithium thickness has been determined, measuring the 478 keV photon count rate allows us to determine the ${}^7\text{Li}(\text{p,p}'\gamma){}^7\text{Li}$ reaction cross-section assuming that the radiation is isotropic; it is shown in Fig. 7. The relative error of the cross-section measurements is determined by the detector count rate error and current stability, and it does not exceed 1%. The absolute cross-section error is determined by the reliability of radionuclide sources of photon radiation (as discussed above, and it does not exceed 15%) and the error in measuring the

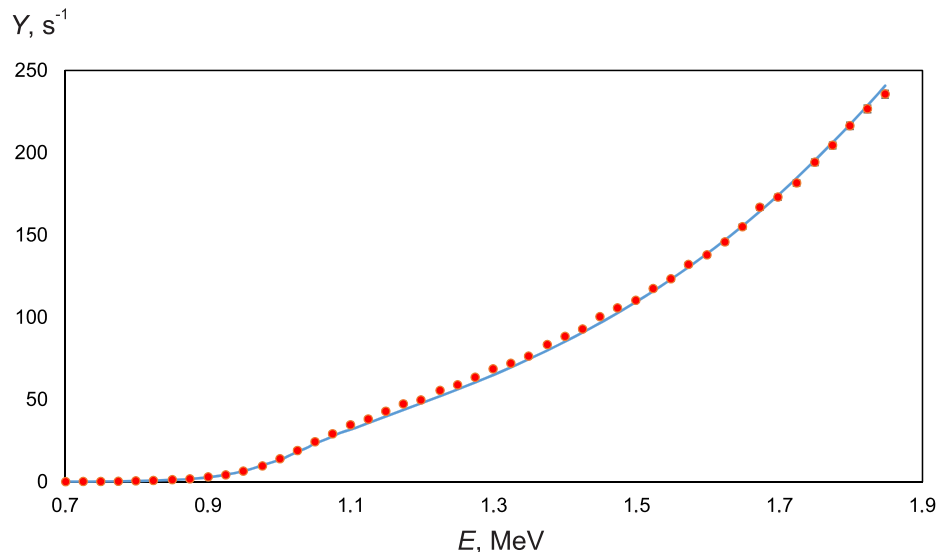


Fig. 6. Dependence of the 478 keV photon count rate on proton energy E : circles – measured from a thick lithium target, line – recovered from measurements from a thin 2.1 μm lithium target.

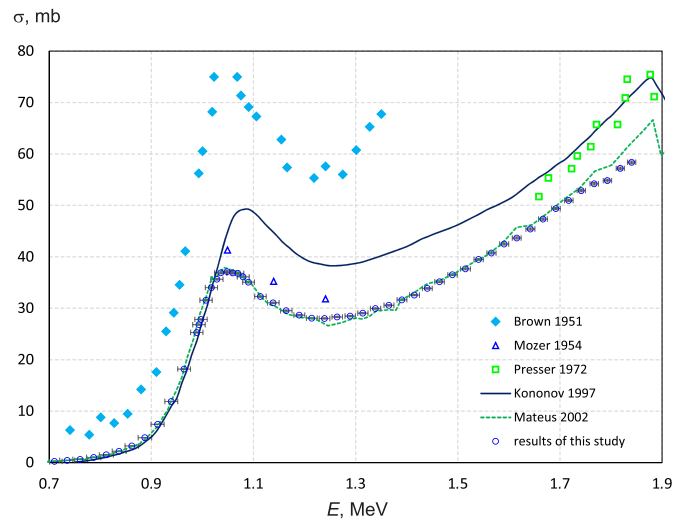


Fig. 7. Cross section of the ${}^7\text{Li}(\text{p,p}'\gamma){}^7\text{Li}$ reaction: \circ – measured in this study. For reference: solid line – (Kononov et al., 1997), \diamond , Δ , \square , dotted line – measurements by (Brown et al., 1951; Mozer et al., 1954; Presser et al., 1972; Mateus et al., 2002). (For interpretation of the references to colour in this figure legend, the reader is referred to the Web version of this article.)

thickness of lithium (1.5%). Although energy stability was better than 0.2%, slowing down of protons in the lithium layer of non-zero thickness increased the error in energy determination, which eventually ranged from 0.4 to 1.2%; it is shown in Fig. 7. Pay attention to the fact that in Figs. 7 and 8 the vertical error bars show only a relative error not exceeding 1%; the absolute error, not shown in the figure, is 15%.

In the article (Aslam et al., 2002), a statement is made that if about 1030 keV resonance peak the radiation is isotropic, then at higher energy it will not. The largest dip in radiation intensity is predicted for an angle of 15° . So, at an energy of 1.8 MeV, the radiation intensity at this angle in the laboratory coordinate system is more than 2 times less than the radiation intensity at an angle of 0° , 90° , or 120° for a thin target and more than 1.3 times less for a thick target. To check the isotropy of the radiation, the measurements were repeated at an angle of 15° . Fig. 8 shows the measured dependences of the radiation intensity at an angle of 15° and 110° from a thin target. It can be seen that no difference from isotropy is observed. The same result was obtained when measuring the

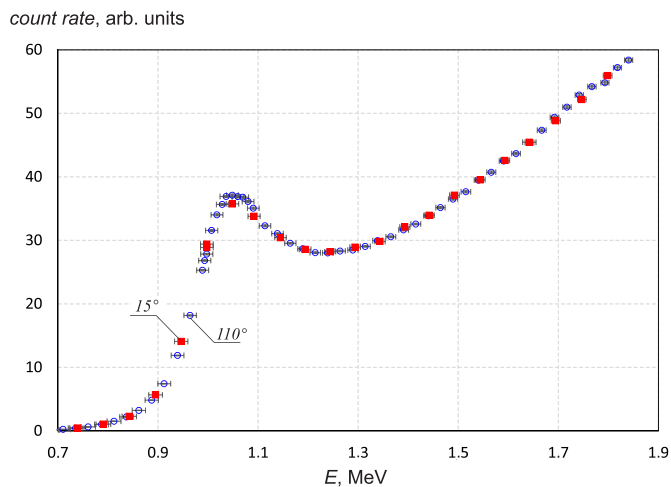


Fig. 8. Measured dependence of the 478 keV photon count rate from a thin lithium target at proton energy E : ○ – emitted at the angle of 110° , □ – 15° .

intensity of radiation from a thick target: an increase in the proton energy from 1.4 to 1.8 MeV increases the radiation intensity by 2.45 ± 0.03 times both at an angle of 110° and 15° , while article (Aslam et al., 2002) predicted an increase in radiation intensity by 1.94 times at an angle of 15° , 3.4 times at an angle of 90° and 3.6 times at an angle of 120° .

Let us compare the obtained result with the previously measured ones (see Fig. 7). The results obtained by Brown in 1951 differ in shape, are strongly overestimated, especially in the area of low energies. V. Kononov's results in 1997 differ in shape, are strongly overestimated in the region of higher energies. Three values presented by Moser in 1954 are systematically overestimated by 14%, which is within the limits of our measurement error. The results of Presser in 1972 are overestimated by 10–20% compared to our measurements. The most recent results of Mateus are almost exactly the same as those obtained by us.

3. Conclusion

For boron neutron capture therapy, a promising technique for the treatment of malignant tumors, an intense epithermal neutron beam with a minimal contribution of accompanying gamma rays is required. It is generally recognized that the optimal reaction of neutron generation is the ${}^7\text{Li}(p,n){}^7\text{Be}$ threshold reaction at proton energy in the 2.3–2.5 MeV region. The knowledge about the ${}^7\text{Li}(p,p'\gamma){}^7\text{Li}$ reaction cross section and 478 keV photon yield is relevant for development of accelerator based neutron sources. The values of photon yield and cross section given in the literature and in the EXFOR database of nuclear reactions differ greatly from one author to another. In this paper, a ${}^7\text{Li}(p,p'\gamma){}^7\text{Li}$ reaction cross section and 478 keV photon yield from a thick lithium target at proton energies from 0.7 to 1.85 MeV were measured with high precision on a vacuum insulated tandem accelerator. The results of previous measurements are analyzed.

Author contributions

Timofey Bykov: software. Dmitrii Kasatov: investigation, writing of the initial draft. Yaroslav Kolesnikov: investigation. Aleksey Koshkarev: data curation. Aleksandr Makarov: validation. Ivan Shchudlo: investigation. Evgeniya Sokolova: formal analysis. Sergey Taskaev: conceptualization, supervision, writing - review & editing.

Declaration of competing interest

The authors declare that they have no known competing financial interests or personal relationships that could have appeared to influence the work reported in this paper.

Acknowledgements

This work was supported by the Russian Science Foundation (project No. 19-72-30005); and the Budker Institute of Nuclear Physics.

References

- Andersen, H., Ziegler, J., 1977. Hydrogen stopping powers and ranges in all elements. In: *Of the Stopping and Ranges of Ions in Matter*, vol. 3. Pergamon Press Inc, Paris. New York, Toronto, Oxford, Sydney, Frankfurt.
- Antilla, A., Hanninen, R., Raisanen, J., 1981. Proton-induced thick-target gamma-ray yields for the elemental analysis of the $Z = 3-9, 11-21$ elements. *Journal of Radioanalytical Chemistry* 62, 293–306. <https://doi.org/10.1007/BF02517360>.
- Aslam, Prestwich, W.V., McNeill, F.E., 2002. Thin target ${}^7\text{Li}(p,p'\gamma){}^7\text{Li}$ inelastic gamma-ray yield measurements. *J. Radioanal. Nucl. Chem.* 254, 533–544. <https://doi.org/10.1023/A:1021646222974>.
- Bayanov, B., Belov, V., Bender, E., Bokhovko, M., Dimov, G., Kononov, V., Kononov, O., Kuksanov, N., Palchikov, V., Pivovarov, V., Salimov, R., Silvestrov, G., Skrinsky, A., Taskaev, S., 1998. Accelerator based neutron source for the neutron-capture and fast neutron therapy at hospital. *Nucl. Instrum. Methods Phys. Res.* 413, 397–426. [https://doi.org/10.1016/S0168-9002\(98\)00425-2](https://doi.org/10.1016/S0168-9002(98)00425-2).
- Bayanov, B., Belov, V., Kindyuk, V., Oparin, E., Taskaev, S., 2004. Lithium neutron producing target for BINP accelerator-based neutron source. *Appl. Radiat. Isot.* 61, 817–821. <https://doi.org/10.1016/j.apradiso.2004.05.032>.
- Bayanov, B., Belov, V., Taskaev, S., 2006. Neutron producing target for accelerator based neutron capture therapy. *J. Phys.: Conf. Series* 41, 460–465. <https://doi.org/10.1088/1742-6596/41/1/051>.
- Bayanov, B., Zhurov, E., Taskaev, S., 2008. Measuring the lithium layer thickness. *Instrum. Exp. Tech.* 51, 147–149. <https://doi.org/10.1134/S002044120801020X>.
- Brown, A.B., Synder, C.W., Fowler, W.A., Lauritsen, C.C., 1951. Excited states of the mirror nuclei, Li^7 and Be^7 . *Phys. Rev.* 82, 159–180. <https://doi.org/10.1103/PhysRev.82.159>.
- IAEA-TECDOC-1223, 2001. *Current Status of Neutron Capture Therapy*. International Atomic Energy Agency, Vienna.
- Kasatov, D., Kolesnikov, I., Koshkarev, A., Makarov, A., Sokolova, E., Shchudlo, I., Taskaev, S., 2020. Method for *in situ* measuring the thickness of a lithium layer. *J. Inst. Met.* 15, P10006. <https://doi.org/10.1088/1748-0221/15/10/P10006>.
- Kononov, V., Bokhovko, M., Kononov, O., Kononova, N., 1997. ${}^7\text{Li}(p,n){}^7\text{Be}$ reaction - based gamma radiation from a neutron source. *Obninsk: Preprint IPPE- 2643*, 10 (in Russian).
- Mateus, R., Jesus, A.P., Braizinha, B., Cruz, J., Pinto, J.V., Ribeiro, J.P., 2002. Proton-induced γ -ray analysis of lithium in thick samples. *Nucl. Instrum. Methods Phys. Res. B* 190, 117–121. [https://doi.org/10.1016/S0168-583X\(01\)01222-8](https://doi.org/10.1016/S0168-583X(01)01222-8).
- Moser, F., Fowler, W.A., Lauritsen, C.C., 1954. Inelastic scattering of protons by Li^7 . *Phys. Rev.* 93, 829–830. <https://doi.org/10.1103/PhysRev.93.829>.
- Presser, G., Bass, R., 1972. Reactions ${}^7\text{Li} + n, {}^7\text{Li} + p$ and excited states of the $A = 8$ system. *Nucl. Phys.* 182, 321–341. [https://doi.org/10.1016/0375-9474\(72\)90281-3](https://doi.org/10.1016/0375-9474(72)90281-3).
- Saito, T., Katabuchi, T., Hales, B., Igashira, M., 2017. Measurement of thick-target gamma-ray production yields of the ${}^7\text{Li}(p,p'){}^7\text{Li}$ and ${}^7\text{Li}(p,\gamma){}^8\text{Be}$ reactions in the near-threshold energy region for the ${}^7\text{Li}(p,n){}^7\text{Be}$ reaction. *J. Nucl. Sci. Technol.* 54, 253–259. <https://doi.org/10.1080/00223131.2016.1255576>.
- Saurwein, W.A.G., Wittig, A., Moss, R., Nakagawa, Y., 2012. *Neutron Capture Therapy: Principles and Applications*. Springer. <https://doi.org/10.1007/978-3-642-31334-9>.
- Savidou, A., Aslanoglou, X., Paradellis, T., Pilakouta, M., 1999. Proton induced thick target γ -ray yields of light nuclei at the energy region $E_p = 1.0\text{--}4.1$ MeV. *Nucl. Instrum. Methods Phys. Res. B* 152, 12–18. [https://doi.org/10.1016/S0168-583X\(98\)00962-8](https://doi.org/10.1016/S0168-583X(98)00962-8).
- Taskaev, S., 2015. Accelerator based epithermal neutron source. *Phys. Part. Nucl.* 46, 956–990. <https://doi.org/10.1134/S1063779615060064>.
- Taskaev, S., 2019. Development of an accelerator-based epithermal neutron source for boron-neutron capture therapy. *Phys. Part. Nucl.* 50, 569–575. <https://doi.org/10.1134/S1063779619050228>.
- Zaidi, L., Belgaid, M., Taskaev, S., Khelifi, R., 2018. Beam shaping assembly design of ${}^7\text{Li}(p,n){}^7\text{Be}$ neutron source for boron neutron capture therapy of deep-seated tumor. *Appl. Radiat. Isot.* 139, 316–324. <https://doi.org/10.1016/j.apradiso.2018.05.029>.